

# UNIVERSITY OF BIRMINGHAM

University of Birmingham  
Research at Birmingham

## Ca<sup>2+</sup> changes in sympathetic varicosities and Schwann cells in rat mesenteric arteries - relation to noradrenaline release and contraction

Hansen, Thomas; Tarasova, Olga S.; Khammy, Makhala M.; Ferreira, Avelino; Kennard, James A.; Andresen, Jørgen; Staehr, C; Brain, Keith; Nilsson, Holger; Aalkjær, Christian

DOI:

[10.1111/apha.13279](https://doi.org/10.1111/apha.13279)

License:

Unspecified

### Document Version

Early version, also known as pre-print

### Citation for published version (Harvard):

Hansen, T, Tarasova, O, Khammy, MM, Ferreira, A, Kennard, JA, Andresen, J, Staehr, C, Brain, K, Nilsson, H & Aalkjær, C 2019, 'Ca<sup>2+</sup> changes in sympathetic varicosities and Schwann cells in rat mesenteric arteries - relation to noradrenaline release and contraction', *Acta Physiologica*, vol. 226, no. 4, e13279. <https://doi.org/10.1111/apha.13279>

[Link to publication on Research at Birmingham portal](#)

### General rights

Unless a licence is specified above, all rights (including copyright and moral rights) in this document are retained by the authors and/or the copyright holders. The express permission of the copyright holder must be obtained for any use of this material other than for purposes permitted by law.

- Users may freely distribute the URL that is used to identify this publication.
- Users may download and/or print one copy of the publication from the University of Birmingham research portal for the purpose of private study or non-commercial research.
- User may use extracts from the document in line with the concept of 'fair dealing' under the Copyright, Designs and Patents Act 1988 (?)
- Users may not further distribute the material nor use it for the purposes of commercial gain.

Where a licence is displayed above, please note the terms and conditions of the licence govern your use of this document.

When citing, please reference the published version.

### Take down policy

While the University of Birmingham exercises care and attention in making items available there are rare occasions when an item has been uploaded in error or has been deemed to be commercially or otherwise sensitive.

If you believe that this is the case for this document, please contact [UBIRA@lists.bham.ac.uk](mailto:UBIRA@lists.bham.ac.uk) providing details and we will remove access to the work immediately and investigate.

# ACTA PHYSIOLOGICA

## [Ca<sup>2+</sup>] changes in sympathetic varicosities and Schwann cells in rat mesenteric arteries – relation to noradrenaline release and contraction

Journal:	<i>Acta Physiologica</i>
Manuscript ID	APH-2018-07-0319.R1
Manuscript Type:	Regular Paper
Date Submitted by the Author:	n/a
Complete List of Authors:	Hansen, Thomas; Aarhus University, Biomedicine Tarasova, Olga; Faculty of Biology, M.V. Lomonosov Moscow State University, Department of Human and Animal Physiology Khammy, Makhala; Aarhus University, Biomedicine Ferreira, Avelino; Aarhus University, Department of Biomedicine Kennard, James; College of Medical and Dental Sciences, University of Birmingham, Institute of Clinical Sciences, Andresen, Joergen; Aarhus University, Biomedicine Staeher, Christian; Aarhus University, Biomedicine Brain, Keith; University of Birmingham, Neuropharmacology and Neurobiology Nilsson, Holger; University of Gothenburg, Institute of Neuroscience and Physiology Aalkjær, Christian; Aarhus University, Biomedicine
Key Words:	amperometry, confocal imaging, neurotransmission, prejunctional modulation, small arteries, sympathetic
Note: The following files were submitted by the author for peer review, but cannot be converted to PDF. You must view these files (e.g. movies) online.	
Suppl. video 1.avi	

1  
2  
3  
4 **[Ca<sup>2+</sup>] changes in sympathetic varicosities and Schwann cells in rat mesenteric arteries –**  
5  
6 **relation to noradrenaline release and contraction**  
7  
8  
9

10  
11 **Thomas Hansen<sup>1</sup>, Olga S. Tarasova<sup>2,3</sup>, Makhala M Khammy<sup>1</sup>, Avelino Ferreira<sup>1</sup>, James A**  
12  
13 **Kennard<sup>4</sup>, Jørgen Andresen<sup>1</sup>, Staehr C<sup>1</sup>, Keith L. Brain<sup>4</sup>, Holger Nilsson<sup>5</sup>, Christian Aalkjær<sup>1</sup>**  
14

15  
16 *<sup>1</sup>Department of Biomedicine, University of Aarhus Denmark*  
17

18 *<sup>2</sup>Faculty of Biology, M.V. Lomonosov Moscow State University, Moscow, Russia*  
19

20 *<sup>3</sup>State Research Center of the Russian Federation - Institute for Biomedical Problems, Moscow,*  
21  
22 *Russia.*  
23

24  
25 *<sup>4</sup>Institute of Clinical Sciences, College of Medical and Dental Sciences, University of Birmingham,*  
26  
27 *UK*  
28

29 *<sup>5</sup>Department of Physiology, Institute of Neuroscience and Physiology, Sahlgrenska Academy at the*  
30  
31 *University of Gothenburg, Sweden*  
32  
33

34  
35  
36  
37  
38 **Short title:** Ca<sup>2+</sup> in sympathetic nerves  
39

40  
41 **Author for correspondence:** Christian Aalkjær, Dept Biomedicine, Aarhus University  
42

43 Ole Worms Alle 4, Aarhus C, Denmark; tel: +45 3045 4306; e-mail: [ca@biomed.au.dk](mailto:ca@biomed.au.dk)  
44  
45  
46  
47  
48  
49  
50  
51  
52  
53  
54  
55  
56  
57  
58  
59  
60

## Abstract

### Aim

This study aimed to assess intracellular  $\text{Ca}^{2+}$  dynamics in nerve cells and Schwann cells in isolated rat resistance arteries and determine how these dynamics modify noradrenaline release from the nerves and consequent force development.

### Methods

$\text{Ca}^{2+}$  in nerves was assessed with confocal imaging, noradrenaline release with amperometry, and artery tone with wire myography.  $\text{Ca}^{2+}$  in axons was assessed after loading with Oregon Green 488 BAPTA-1 dextran. In other experiments, arteries were incubated with Calcium Green-1-AM which loads both axons and Schwann cells.

### Results

Schwann cells but not axons responded with a  $\text{Ca}^{2+}$  increase to ATP. Electrical field stimulation of nerves caused a frequency dependent increase of varicose  $[\text{Ca}^{2+}]_v$  ( $[\text{Ca}^{2+}]_v$ ).  $\omega$ -conotoxin-GVIA (100 nM) reduced the  $[\text{Ca}^{2+}]_v$  transient to 2 Hz and 16 Hz by 60% and 27%, respectively; in contrast  $\omega$ -conotoxin GVIA inhibited more than 80% of the noradrenaline release and force development at 2 and 16 Hz. The  $\text{K}_v$  channel blocker, 4-aminopyridine (10  $\mu\text{M}$ ), increased  $[\text{Ca}^{2+}]_v$ , noradrenaline release, and force development both in the absence and presence of  $\omega$ -conotoxin-GVIA. Yohimbine (1  $\mu\text{M}$ ) increased both  $[\text{Ca}^{2+}]_v$  and noradrenaline release but reduced force development.

Acetylcholine (10  $\mu\text{M}$ ) caused atropine-sensitive inhibition of  $[\text{Ca}^{2+}]_v$ , noradrenaline release and force. In the presence of  $\omega$ -conotoxin-GVIA, acetylcholine caused a further inhibition of all parameters.

### Conclusion

Modification of  $[\text{Ca}^{2+}]$  in arterial sympathetic axons and Schwann cells was assessed separately.  $\text{K}_v3.1$  channels may be important regulators of  $[\text{Ca}^{2+}]_v$ , noradrenaline release, and force

1  
2  
3  
4 development. Presynaptic adrenoceptor and muscarinic receptor activation modify transmitter  
5  
6 release through modification of  $[Ca^{2+}]_v$ .  
7  
8  
9

10  
11 **Keywords**  
12

13 Amperometry, confocal imaging, neurotransmission, prejunctional modulation, small arteries,  
14  
15 sympathetic.  
16  
17  
18  
19  
20  
21  
22  
23  
24  
25  
26  
27  
28  
29  
30  
31  
32  
33  
34  
35  
36  
37  
38  
39  
40  
41  
42  
43  
44  
45  
46  
47  
48  
49  
50  
51  
52  
53  
54  
55  
56  
57  
58  
59  
60

For Peer Review

## INTRODUCTION

Sympathetic nerves are important regulators of resistance artery tone. Extensive information on the pharmacology of transmitter release and transmitter effect in the vascular wall has accumulated over many years. This pharmacological characterization combined with evidence from other tissues suggest that the concentration of  $\text{Ca}^{2+}$  in the varicosities ( $[\text{Ca}^{2+}]_v$ ) is important for transmitter release. It is also well known that several presynaptic receptors modify transmitter release and that pharmacological modification of ion channel activity can modify the release. Remarkably, however, there is no direct information on  $[\text{Ca}^{2+}]_v$  in the vascular sympathetic nerves and therefore no direct information as to whether, for example, presynaptic receptors or ion channel activity modify transmitter release through modification of  $[\text{Ca}^{2+}]_v$ . This is largely because the small size of the terminal branches of the sympathetic axons and the varicosities (which typically have diameters around  $1 \mu\text{m}$ ) and the presence of Schwann cells<sup>1</sup> make it difficult to directly assess  $[\text{Ca}^{2+}]_v$  and other second messengers in the varicosities.

In this study we have applied  $\text{Ca}^{2+}$ -sensitive dyes, amperometry and myography to assess the relationship between  $[\text{Ca}^{2+}]_v$ , intracellular  $\text{Ca}^{2+}$  concentration ( $[\text{Ca}^{2+}]_i$ ) in axons and Schwann cells, noradrenaline (NA) release, and force development in rat resistance arteries. Because we wanted to assess both  $[\text{Ca}^{2+}]_v$  in axons and  $[\text{Ca}^{2+}]_i$  in Schwann cells we used two calcium dye loading protocols. To ensure selective dye loading of axons, we used a protocol developed for selective loading of axons in vas deferens<sup>2-5</sup>. To load axons and Schwann cells simultaneously we used the traditional loading of a lipophilic  $\text{Ca}^{2+}$  sensitive dye.

We have characterized the effect of known modulators of NA release on  $[\text{Ca}^{2+}]_v$  and related this to their effects on NA release and force development, and evaluated the differential effect of ATP on

1  
2  
3  
4  $[Ca^{2+}]_v$  and Schwann cell  $[Ca^{2+}]_i$ . We compared our  $[Ca^{2+}]_v$  data with  $[Ca^{2+}]_v$  data obtained in the  
5  
6 sympathetic nerve terminals of vas deferens <sup>2-5</sup>.  
7  
8  
9

## 10 11 RESULTS

12  
13  
14  
15  *$[Ca^{2+}]_i$  transients in nerve fibers loaded with Calcium Green-AM.*

16  
17 Following loading of Calcium Green-AM, nerve fibers were easily seen (Fig. 1A) lying  
18 immediately outside the smooth muscle cells. The pattern seen after loading with Calcium Green-  
19 AM was similar to the pattern seen after staining with the catecholamine-specific stain glyoxylic  
20 acid (Suppl. Fig 1) consistent with the structures stained with Calcium Green-AM are nerve fibers  
21 (i.e. axons and Schwann cells). It was not possible to distinguish varicosities. With field stimulation  
22 a frequency-dependent increase in  $[Ca^{2+}]_i$  was seen (Fig. 1B), which was TTX sensitive (insert Fig  
23 1B). At low frequencies the effect of individual stimuli could be discerned, and a cumulative  
24 increase of  $[Ca^{2+}]_i$  consequent to a slow net decrease of the  $[Ca^{2+}]_i$  transient was apparent (Fig. 1B).  
25 Where  $\geq 3$  nerve fibers crossed, the fluorescence was often bright (single arrow in Fig. 1A). In 20-  
26 30% of these crossings, the nuclear stain Syto16 revealed the presence of nuclei in the nerve fiber  
27 (Fig. 1C, 1D and Suppl. Video 1).  
28  
29  
30  
31  
32  
33  
34  
35  
36  
37  
38  
39  
40  
41  
42

43 The increase of  $[Ca^{2+}]_i$  to 2 and 16 Hz stimulation is seen in nerve fibers (Fig. 1E) and in areas  
44 where nerve fibers cross (Fig. 1F) though the increase in  $[Ca^{2+}]_i$  at both 2 Hz and 16 Hz was small  
45 in areas where nerve fibers cross. Prior incubation with 10  $\mu$ M ATP did not significantly increase  
46 the response to field stimulation in either of these areas (Fig. 1E and 1F). In non-activated arteries  
47 10  $\mu$ M ATP caused a substantial increase of  $[Ca^{2+}]_i$  in the area where nerve fibers cross (Fig. 2,  
48 column 2). In the nerve fibers outside the crossing areas the increase did not obtain statistical  
49 significance (Fig. 2, column 1).  
50  
51  
52  
53  
54  
55  
56  
57  
58  
59  
60

1  
2  
3  
4  
5  
6  
7 The increase in  $[Ca^{2+}]_i$  with field stimulation was partly inhibited by 100 nM of the N-type  $Ca^{2+}$   
8 channel blocker  $\omega$ -conotoxin GVIA (Fig. 3). The L-type  $Ca^{2+}$  channel blocker nifedipine (0.3  $\mu$ M)  
9 and the predominantly T-type  $Ca^{2+}$  channel blocker mibefradil (1  $\mu$ M) were without effect on  
10  $[Ca^{2+}]_i$  (the fluorescence relative to the time control value were  $1.02 \pm 0.02$  and  $1.01 \pm 0.01$  for  
11 nifedipine and mibefradil, respectively,  $n=7$ ). However, both 0.3  $\mu$ M nifedipine and 1  $\mu$ M  
12 mibefradil reduced the force response to stimulation with exogenous NA (with tension relative to  
13 the time control tension of  $5 \pm 1\%$  and  $4 \pm 1\%$  for nifedipine and mibefradil, respectively,  $n=7$ ),  
14 indicating that they were used in relevant concentrations. The  $\omega$ -conotoxin GVIA insensitive  
15 component of the  $[Ca^{2+}]_i$  response to field stimulation increased with increasing frequencies and  
16 only about 40% of the  $[Ca^{2+}]_i$  response to 16 Hz stimulation was inhibited by  $\omega$ -conotoxin GVIA  
17 (Fig. 3).  
18  
19  
20  
21  
22  
23  
24  
25  
26  
27  
28  
29  
30  
31  
32  
33

#### 34 *$[Ca^{2+}]_i$ transients in axons loaded with Oregon Green 488 BAPTA-1 dextran*

35  
36  
37  
38

39 In arterial segments loaded through the suction pipette with Oregon Green 488 BAPTA-1 dextran,  
40 varicosities and intervaricose segments were easily distinguished (Fig. 4A) while, as expected,  
41 extracellular structures, smooth muscle cells or endothelial cells were not seen.  
42  
43  
44  
45  
46  
47

48 Field stimulation resulted in a frequency-dependent increase in  $[Ca^{2+}]_v$  (Fig. 4B). With Oregon  
49 Green 488 BAPTA dextran loading, the transient increase in  $[Ca^{2+}]_v$  to a single electrical pulse had  
50 a higher amplitude and a faster decline than the  $[Ca^{2+}]_i$  transient seen after Calcium Green-AM  
51 loading (Fig. 4C). The  $[Ca^{2+}]_v$  transients were fully inhibited by 100 nM TTX at all stimulation  
52 frequencies (data not shown).  
53  
54  
55  
56  
57  
58  
59  
60



1  
2  
3  
4  
5  
6  
7 Addition of ATP caused a significant reduction of the  $[Ca^{2+}]_v$  amplitude to 2 Hz and 16 Hz (Fig.  
8  
9 4D). In contrast to what was seen with Calcium Green AM loaded arteries, ATP did not increase  
10  
11 baseline  $[Ca^{2+}]_v$  (Fig. 2, bar labeled Oregon Green).  
12  
13  
14

#### 15 16 *Effect of pharmacological interventions on $[Ca^{2+}]_v$ , noradrenaline release, and force*

17  
18 We assessed whether presynaptic pharmacological intervention modified NA release and force via  
19  
20 an effect on  $[Ca^{2+}]_v$ . Fig. 5 shows traces from an experiment where NA release and force were  
21  
22 assessed. Fig. 6 shows the mean values for the frequency-response curves for  $[Ca^{2+}]_v$ , NA release,  
23  
24 and force. Based on these data it was decided to concentrate on stimulation with 2 Hz and 16 Hz.  
25  
26 The drugs used in these experiments did not affect  $[Ca^{2+}]_v$ , NA, or force under baseline conditions  
27  
28 (i.e. before the stimulation).  
29  
30  
31  
32  
33

#### 34 *$Ca^{2+}$ channel inhibition with $\omega$ -conotoxin GVIA.*

35  
36 The effect of  $\omega$ -conotoxin GVIA on  $[Ca^{2+}]_v$  was frequency-dependent and a larger proportion of  
37  
38 the  $[Ca^{2+}]_v$  response was inhibited at low frequencies compared to higher frequencies (Fig. 7A)  
39  
40 similarly to what we observed for  $[Ca^{2+}]_i$  after Calcium Green AM loading. To assess whether 100  
41  
42 nM  $\omega$ -conotoxin GVIA was a supramaximal concentration, inhibition of  $[Ca^{2+}]_v$  transient with 100  
43  
44 nM and 300 nM  $\omega$ -conotoxin GVIA was compared. No additional effect of 300 nM  $\omega$ -conotoxin  
45  
46 GVIA was seen (the response remaining to 16 Hz stimulation was  $74\pm 8\%$  and  $71\pm 7\%$  in the  
47  
48 presence of 100 and 300 nM  $\omega$ -conotoxin GVIA, respectively,  $n=4$ , n.s. paired Student t-test). In  
49  
50 contrast 100 nM  $\omega$ -conotoxin GVIA inhibited more than 80% of the NA release and force  
51  
52 development (Fig. 7B and 7C) while having no effect on force development to exogenously applied  
53  
54 NA (Fig. 8).  
55  
56  
57  
58  
59  
60

### *K<sup>+</sup> channel inhibition.*

In the presence of 10  $\mu\text{M}$  4-AP, the field stimulation elicited  $[\text{Ca}^{2+}]_v$  transient, NA release and force development all increased (Fig. 7), while 10  $\mu\text{M}$  4-AP had no effect on force development to exogenously applied NA (Fig. 8). In the presence of  $\omega$ -conotoxin GVIA, 4-AP still increased the responses (Fig. 7). To assess whether 10  $\mu\text{M}$  4-AP was sufficient to cause full effect, NA release and force at 16 Hz was assessed with 10  $\mu\text{M}$ , 100  $\mu\text{M}$ , and 200  $\mu\text{M}$  4-AP. The potentiation elicited with 100  $\mu\text{M}$  4-AP was greater than elicited with 10  $\mu\text{M}$  4-AP; with 200  $\mu\text{M}$  4-AP no further potentiation of NA release and force was seen (Fig. 9). The effect of 4-AP on tension development to 16 Hz was similar to the effect on NA release. To further characterize the  $\text{K}^+$ -channels affected by 4-AP, the effects of charybdotoxin, TEA, and dendrotoxin were assessed. Charybdotoxin (100 nM) had no effect on NA release (Fig. 9B) but potentiated the tension response to 16 Hz. TEA (0.5 mM in the presence of charybdotoxin) increased the release of NA to the same extent as 100  $\mu\text{M}$  4-AP. TEA at 1 and 2 mM caused a further increase in NA release. The effects of TEA on the tension response to 16 Hz was similar to the effect on NA release. Dendrotoxin (0.1  $\mu\text{M}$ ) had no effect on field stimulation-induced force generation (2 Hz:  $0.31 \pm 0.07 \text{ Nm}^{-1}$  and  $0.26 \pm 0.05 \text{ Nm}^{-1}$  and 16 Hz:  $2.71 \pm 0.41 \text{ Nm}^{-1}$  and  $2.19 \pm 0.36 \text{ Nm}^{-1}$ , control and dendrotoxin, respectively ( $n=8$  and 8)). **These experiments were made with 5.9 mM extracellular  $\text{K}^+$ . We also determined the effect of 10  $\mu\text{M}$  4-AP and 0.1  $\mu\text{M}$  dendrotoxin at 3 mM  $\text{K}^+$ . Also at the lower  $\text{K}^+$  concentration 4-AP increased the NA release to 16 Hz field stimulation ( $293 \pm 49 \%$ ,  $n=3$ ), while dendrotoxin was without effect ( $126 \pm 28\%$ ,  $n=3$ ).**

### *$\alpha$ -Adrenoceptor inhibition with yohimbine.*

In the presence of yohimbine (1  $\mu\text{M}$ )  $[\text{Ca}^{2+}]_v$  and NA release increased (Fig. 7A and 7B) but force development was inhibited (Fig. 7C). In the presence of  $\omega$ -conotoxin GVIA, yohimbine had no

1  
2  
3  
4 effect on  $[Ca^{2+}]_v$  transients and NA release but did inhibit the force response at 16 Hz (Fig. 7). In  
5  
6 the presence of 200  $\mu$ M 4-AP or 2 mM TEA, yohimbine had no effect on NA release (Fig. 9) or  
7  
8 tension response to 16 Hz. Yohimbine caused a rightward-shift of the concentration-force curve to  
9  
10 exogenously applied NA (Fig. 8).  
11  
12  
13  
14

#### 15 *ACh receptor activation with ACh.*

16  
17 ACh (20  $\mu$ M) caused inhibition of  $[Ca^{2+}]_v$ , NA release and tension at both 2 Hz and 16 Hz (Fig. 7).  
18  
19 In the presence of  $\omega$ -conotoxin GVIA, ACh caused a further inhibition of  $[Ca^{2+}]_v$ , NA release and  
20  
21 tension (Fig. 7). ACh caused a rightward shift of the concentration-force curve to exogenously  
22  
23 applied NA (Fig. 8). The effects of ACh on NA release and force were prevented by application of  
24  
25 1  $\mu$ M atropine ( $n=4$ , data not shown).  
26  
27  
28  
29  
30  
31

## 32 **DISCUSSION**

33  
34  
35  
36 Despite its critical importance for control of vascular tone no direct measurements have been made  
37  
38 of the intravariocose signaling that leads to transmitter release or modifies transmitter release  
39  
40 following depolarization of vascular sympathetic nerves. In this study we assessed  $Ca^{2+}$  transients in  
41  
42 varicosities using a fluorescent dye technique that specifically loads axons of perivascular nerves.  
43  
44 Using a different protocol for dye loading we also assessed  $Ca^{2+}$  transients in nerve fibers which  
45  
46 include axons and Schwann cells.  
47  
48  
49  
50  
51

52 In one approach, we applied Calcium Green-AM, which is expected to load both Schwann cells and  
53  
54 axons. In the second approach, we exposed the cut vessel ends to Oregon Green 488 BAPTA-1  
55  
56 dextran. The latter technique exploits an axonal transport system present in nerves to transport the  
57  
58  
59  
60

1  
2  
3  
4 dye to downstream axons that have not been in direct contact with the dye. Images in the  
5  
6 downstream areas therefore reflect calcium in axons only. This was confirmed by several  
7  
8 observations. Calcium Green-AM loading led to images of relatively thick nerves with a fuzzy  
9  
10 appearance and with characteristic areas of high fluorescence intensity in areas where nerve fibers  
11  
12 crossed. This contrasts with the sharply defined, thin fibers with distinct varicosities following  
13  
14 Oregon Green 488 BAPTA-1 dextran loading. Staining with the nuclear dye Syto16 revealed that  
15  
16 the areas of high Calcium Green fluorescence intensity often were **contained** nuclei. As cell nuclei  
17  
18 present in nerve fibers are Schwann cell nuclei, our observations suggest that Schwann cell somas  
19  
20 often locate to areas where nerve fibers cross. It will be relevant in further ultrastructural and  
21  
22 stereological studies to test this conclusion. Additional evidence that the areas with high dye  
23  
24 intensity are Schwann cells comes from the finding that ATP causes a substantial increase in  $[Ca^{2+}]_i$   
25  
26 in these areas while field stimulation causes only small increases in  $[Ca^{2+}]_i$ . The response to ATP  
27  
28 confirms that the limited response to field stimulation in these areas is not due to dye saturation.  
29  
30 Notably, ATP did not increase fluorescence when axons were loaded with Oregon Green 488  
31  
32 BAPTA-1 dextran. Schwann cells in the sympathetic nerves respond to ATP with an increase of  
33  
34  $[Ca^{2+}]_i$ <sup>6,7</sup>, so our data strongly suggests that Schwann cells take up Calcium Green-AM and that  
35  
36  $[Ca^{2+}]_i$  changes following intervention reflect Schwann cell function. We suggest that Schwann cell  
37  
38 pharmacology can be assessed by imaging these areas following Calcium Green-AM loading.  
39  
40  
41  
42  
43  
44  
45  
46  
47

48 The Calcium Green-AM loaded nerves fibers outside the areas where nerve fibers cross responded  
49  
50 with an increase of  $[Ca^{2+}]_i$  to field stimulation in a frequency-dependent manner. Several  
51  
52 observations suggest that these responses are dominated by the axons; 1) the responses were  
53  
54 reminiscent of the response in the Oregon Green 488 BAPTA-1 dextran loaded arteries with minor  
55  
56 quantitative differences (i.e. a slower transient), 2) the responses to electrical stimulation were small  
57  
58  
59  
60

1  
2  
3  
4 in the areas of the putative Schwann cell body, 3) the N-type calcium channel blocker  $\omega$ -conotoxin  
5  
6 GVIA had similar effects in Oregon Green 488 BAPTA-1 dextran and Calcium Green-AM loaded  
7  
8 arteries, 4) blockers of L-type and T-type calcium channels, which are expressed in Schwann cells<sup>8</sup>  
9  
10 were without effect in the Calcium Green-AM loaded arteries, and 5) the responses were TTX-  
11  
12 sensitive.  
13  
14

15  
16  
17  
18 Following Oregon Green 488 BAPTA-1 dextran loading the axons responded with a frequency-  
19  
20 dependent increase of  $[Ca^{2+}]_i$ . Both  $[Ca^{2+}]_i$  in the intervaricose segments and  $[Ca^{2+}]_v$  increased to  
21  
22 field stimulation and the responses were fully inhibited with TTX, confirming their expected  
23  
24 dependence on TTX-sensitive voltage-gated  $Na^+$  channels.  
25  
26

27  
28  
29 N-type  $Ca^{2+}$  channel inhibition only partly reduced the  $Ca^{2+}$  increase in the axons. Even at low  
30  
31 stimulation frequencies, when  $\omega$ -conotoxin GVIA was most effective, a substantial part of the field  
32  
33 stimulation-induced  $[Ca^{2+}]_v$  increase remained. We routinely used 100 nM  $\omega$ -conotoxin GVIA.  
34  
35 Application of 300 nM did not cause any further inhibition of  $[Ca^{2+}]_v$  indicating that the remaining  
36  
37  $[Ca^{2+}]_v$  increase is unlikely to be via incompletely blocked N-type  $Ca^{2+}$  channels. A similar inability  
38  
39 of  $\omega$ -conotoxin GVIA to fully block the  $[Ca^{2+}]_v$  increase to field stimulation has been reported for  
40  
41 vas deferens<sup>2,4</sup>. We do not know which pathway is important for the remaining  $[Ca^{2+}]_v$  increase.  
42  
43 Given that it was not blocked with nifedipine and mibefradil it is unlikely to be mediated by L-type  
44  
45 and T-type calcium channels. In the vas deferens, Brain and Bennett (1997) found that the  $[Ca^{2+}]_v$   
46  
47 increase remaining after  $\omega$ -conotoxin GVIA was also insensitive to 100 nM of the P/Q-type  $Ca^{2+}$   
48  
49 channel blocker,  $\omega$ -agatoxin TK. It will be important to determine the source of  $Ca^{2+}$  responsible  
50  
51 for the  $\omega$ -conotoxin GVIA -insensitive increase of  $[Ca^{2+}]_v$  and determine its physiological  
52  
53 importance. In contrast to the effect of 100 nM  $\omega$ -conotoxin GVIA on  $Ca^{2+}$ , 100 nM  $\omega$ -conotoxin  
54  
55  
56  
57  
58  
59  
60

1  
2  
3  
4 GVIA almost completely inhibited NA release and force development. This could suggest a steep  
5  
6 relationship between  $[Ca^{2+}]_v$  and NA release. Against this possibility is the finding that in the  
7  
8 presence of 4-AP and  $\omega$ -conotoxin GVIA  $[Ca^{2+}]_v$  is very close to normal levels while NA release is  
9  
10 substantially reduced. The alternative possibility, that a substantial part of the  $Ca^{2+}$  increase in the  
11  
12 varicosities during field stimulation is irrelevant for NA release, is therefore more likely.

13  
14  
15 The voltage-gated  $K^+$ -channel inhibitor 4-AP is reported to increase transmitter release in the  
16  
17 vascular wall <sup>9,10</sup>. 4-AP is expected to modify the action potential and consequently enhance the  
18  
19  $[Ca^{2+}]_v$  increase; this has been observed with 10 mM 4-AP in the vas deferens <sup>4</sup>. We found in the  
20  
21 vascular wall that 10  $\mu$ M 4-AP led to a significant increase of  $[Ca^{2+}]_v$  associated with an increase of  
22  
23 NA release and force development. 4-AP not only increased the  $\omega$ -conotoxin GVIA-sensitive  
24  
25 component but also the  $\omega$ -conotoxin GVIA-insensitive component, which suggests that the  $\omega$ -  
26  
27 conotoxin GVIA-insensitive  $[Ca^{2+}]_v$  increase is controlled by the membrane potential and at least in  
28  
29 part can contribute to NA release. At 10  $\mu$ M, 4-AP had, as expected, no effect on the force  
30  
31 development to exogenously applied NA, and the increased tension during field stimulation can be  
32  
33 explained by the effect on NA release. The effect of 10  $\mu$ M 4-AP on  $[Ca^{2+}]_v$ , NA release and force  
34  
35 development is consistent with the finding that 10  $\mu$ M 4-AP also increases <sup>3</sup>H-noradrenaline  
36  
37 overflow from the rabbit tail artery <sup>10</sup> and that 20  $\mu$ M 4-AP blocks the endothelin-mediated  
38  
39 inhibition of NA release from gastric nerves <sup>11</sup>. Since 100  $\mu$ M 4-AP produced a maximal effect, the  
40  
41  $K_V3.1$  channel, which is the only channel with an  $IC_{50}$  for 4-AP below 100  $\mu$ M <sup>12,13</sup>, is the most  
42  
43 likely channel candidate.  $K_V1$  channels are suggested to be important in varicosities in vas deferens  
44  
45 <sup>4</sup>, but  $K_V1$  channels have an  $IC_{50}$  for 4-AP of  $\geq 160$   $\mu$ M <sup>13</sup> and are therefore less likely candidates in  
46  
47 perivascular nerves. To further test the potential role of  $K_V1$  we used 100 nM dendrotoxin, which  
48  
49 effectively blocks  $K_V1$  channels <sup>13</sup>. The lack of effect of dendrotoxin further supports  $K_V3.1$   
50  
51 channels as the most likely candidate. The effect of 4-AP and lack of effect of dendrotoxin was seen  
52  
53  
54  
55  
56  
57  
58  
59  
60

1  
2  
3  
4 at 5.9 mM extracellular  $K^+$  as well as the 3 mM  $K^+$  which is a more physiological  $K^+$  concentration.  
5  
6  $K_v3.1$  channels are sensitive to TEA at sub-mM concentrations <sup>13</sup>. Our finding that 0.5 mM TEA  
7  
8 enhanced NA release and force development to the same extent as 200  $\mu$ M 4-AP further supports a  
9  
10 role for  $K_v3.1$  channels. However, since 1 and 2 mM TEA had additional effects on NA release and  
11  
12 force development, other  $K^+$ -channels are likely to be important in the vascular varicosity: these are  
13  
14 unlikely to be  $BK_{Ca}$  channels since charybdotoxin was without effect.  
15  
16  
17  
18  
19

20 Several presynaptic receptors modify transmitter release, although their mechanisms of action are  
21  
22 not clear. We have assessed the signaling from cholinergic, adrenergic, and purinergic receptors.  
23  
24 ACh caused a modest reduction of  $[Ca^{2+}]_v$ , particularly at 16 Hz, but a strong inhibition of NA  
25  
26 release and force, mediated by muscarinic receptors. These effects were reminiscent of the effect of  
27  
28  $\omega$ -conotoxin GVIA, and it seems likely that ACh works through inhibition of  $\omega$ -conotoxin GVIA-  
29  
30 sensitive  $Ca^{2+}$  influx. However, ACh added in the presence of  $\omega$ -conotoxin GVIA caused a further  
31  
32 reduction of  $[Ca^{2+}]_v$ , suggesting that ACh may also partly decrease the  $\omega$ -conotoxin GVIA-  
33  
34 insensitive increase of  $[Ca^{2+}]_v$ . The data reinforces the possibility that NA release can be modified  
35  
36 through mechanisms independent of  $\omega$ -conotoxin GVIA-sensitive  $Ca^{2+}$  influx. As expected, ACh  
37  
38 also reduced force to exogenously applied NA, probably via an endothelium dependent mechanism.  
39  
40 Therefore, the effect of ACh on field stimulation induced force development is difficult to interpret.  
41  
42  
43 Yohimbine, which is predominantly an  $\alpha_2$ -adrenoceptor antagonist, increased field stimulation-  
44  
45 induced  $[Ca^{2+}]_v$  increase and NA release, suggesting that presynaptic  $\alpha_2$ -adrenoceptor-mediated  
46  
47 negative feedback of NA release signals through reduction of  $[Ca^{2+}]_v$ . Furthermore, since  
48  
49 yohimbine had no effect on NA release in the presence of 4-AP or TEA, the presynaptic  $\alpha_2$ -  
50  
51 adrenoceptors most likely inhibits NA release via activation of  $K_v3.1$  channels. Despite the  
52  
53 yohimbine induced potentiation of field stimulation-induced increase of  $[Ca^{2+}]_v$  and NA release,  
54  
55  
56  
57  
58  
59  
60

1  
2  
3  
4 yohimbine inhibited force development. Yohimbine also reduced the sensitivity to exogenously  
5  
6 applied NA. This is despite the fact that smooth muscle cells of rat mesenteric small arteries only  
7  
8 have  $\alpha_1$ -adrenoceptors <sup>14</sup>, suggesting that 1  $\mu$ M yohimbine may also inhibits  $\alpha_1$ -adrenoceptors in  
9  
10 this preparation <sup>15</sup>. We also found an inhibitory effect of ATP on the  $[Ca^{2+}]_v$  increase to field  
11  
12 stimulation. It will be of interest to determine whether this is mediated via presynaptic P2Y  
13  
14 receptors, as suggested for the sympathetic terminals of the mouse vas deferens <sup>5</sup>.  
15  
16  
17  
18  
19

### 20 *Conclusion*

21  
22 In this study we have made a pharmacological characterization of  $Ca^{2+}$  homeostasis in varicosities  
23  
24 and Schwann cells in the vascular wall and compared this to NA release and force development. We  
25  
26 confirmed that Schwann cells respond with a  $[Ca^{2+}]_i$  increase to ATP. This contrast with  
27  
28 varicosities, where a decrease of the  $[Ca^{2+}]_v$  transient to field stimulation is seen. Our data further  
29  
30 suggests that a large part of the electrical field induced increase of  $[Ca^{2+}]_v$  is irrelevant for NA  
31  
32 release. The pharmacological analysis suggests that  $K_v3.1$  is an important regulator of  $[Ca^{2+}]_v$ , NA  
33  
34 release and force and suggest that both presynaptic adrenoceptors and muscarinic receptors modify  
35  
36 transmitter release through effects on  $[Ca^{2+}]_v$ .  
37  
38  
39  
40  
41  
42

### 43 **MATERIALS AND METHODS**

44  
45  
46  
47  
48 *Animals.* Male Wistar rats (16-19 weeks) were used. The investigation conforms to the Guide for  
49  
50 the Care and Use of Laboratory Animals published by the US National Institutes of Health (NIH  
51  
52 Publication No. 85-23, revised 1996) as well as the guidelines from Directive 2010/63/EU of the  
53  
54 European Parliament and Danish national guidelines for animal research. Rats were anesthetized  
55  
56  
57  
58  
59  
60



1  
2  
3  
4 with CO<sub>2</sub> inhalation and killed by decapitation. Branches (2<sup>nd</sup> and 3<sup>rd</sup> order) of the mesenteric artery  
5  
6 were dissected out; the arteries had inner diameters of 200-250 μm.  
7  
8  
9

10  
11 *Mounting and normalization of artery segments in myographs for isometric force recordings.* For  
12  
13 Ca<sup>2+</sup> imaging 2-mm-long artery segments were mounted as rings in a myograph (360CW, Danish  
14  
15 Myo Technology A/S, Denmark) for simultaneous recording of isometric force and confocal  
16  
17 imaging as described previously <sup>16</sup>. Force transducer readings were recorded at 100 Hz using  
18  
19 PowerLab and LabChart (ADInstruments, New Zealand).  
20  
21  
22

23  
24 A passive tension-length curve was obtained and the arteries set, based on the passive tension-  
25  
26 length curve, to a value where near-maximal active force is developed <sup>17</sup>. After equilibration in  
27  
28 physiological salt solution (PSS; for composition see below) at 37°C for about 1 hour, the arteries  
29  
30 were activated twice with 10 μM NA in PSS. The relaxed artery was then stimulated after one of  
31  
32 several protocols. The basis for the protocols was a series of square-wave field stimulations from  
33  
34 platinum electrodes placed in the mounting heads of the myograph as described previously <sup>18</sup>.  
35  
36 Stimulations were with electrical pulses with pulse width between 0.2 and 0.4 ms and a current  
37  
38 strength of 40 mA. The pulses had frequencies from 0.5 to 16 Hz and were run for 3 s at each  
39  
40 frequency. **These frequencies were chosen because 1-2 Hz is the physiologically most relevant**  
41  
42 **frequency<sup>19</sup> and 16 Hz gives the maximal nerve-specific activation in this preparation<sup>20</sup>.** An interval  
43  
44 of 3 minutes was used between the different frequencies. In some protocols the arteries were  
45  
46 stimulated only at 2 Hz and/or 16 Hz each for 3 s but otherwise using the same stimulation  
47  
48 parameters. The arteries were incubated with drugs for 15 minutes before the electrical field  
49  
50 stimulations were initiated. The drugs were used in the following concentrations: ω-conotoxin  
51  
52 GVIA (CTX) 100 nM and 300 nM, 4-aminopyridine (4-AP) 10 μM, 100 μM, and 200 μM;  
53  
54  
55  
56  
57  
58  
59  
60

1  
2  
3  
4 tetraethylammonium (TEA) 0.5 mM, 1 mM, and 2 mM; tetrodotoxin (TTX) 0.1  $\mu$ M; dendrotoxin  
5 0.1  $\mu$ M; charybdotoxin 0.1  $\mu$ M; yohimbine 1  $\mu$ M; ACh 20  $\mu$ M and cocaine 3  $\mu$ M. In some  
6  
7  
8 experiments, exogenous NA and ATP effects were assessed.  
9

10  
11  
12  
13 *Loading of nerve fibers.* After mounting and normalization of an artery segment in a myograph the  
14 artery was incubated with 5  $\mu$ M of the  $\text{Ca}^{2+}$ -sensitive dye Calcium Green-1-AM in PSS for two  
15  
16  
17 times 1.5 hours at 37°C.  
18  
19

20  
21  
22  
23 *Axon-specific loading.* A 3-4 mm long artery segment was dissected. The proximal end of the artery  
24 was secured in a glass suction pipette filled with phosphate-free PSS (for composition see below)  
25 containing 43 mM Oregon Green 488 BAPTA-1 10 kDa dextran. The distal part of the artery was  
26  
27  
28 kept in PSS. The solution remained at room temperature and the segments were loaded for 5-6  
29  
30  
31 hours. Thereafter the artery was released from the glass suction pipette and maintained in PSS for a  
32  
33  
34 minimum of 3 hours at room temperature, after which the segment was mounted in a myograph as  
35  
36  
37 described above.  
38  
39

40  
41 *Imaging.* Imaging of  $\text{Ca}^{2+}$  in axons and nerve fibers was made with either a Noran Odyssey  
42  
43  
44 confocal unit mounted on a Nikon Inverted Microscope Eclipse TE2000-U with a 60 $\times$ , water  
45  
46  
47 dipping objective or a Zeiss Axiovert 200M confocal microscope with a 40 $\times$  water dipping  
48  
49  
50 objective. The excitation was from the 488 nm line of an argon laser, a dichroic mirror of 505 nm  
51  
52  
53 was used and on the emission side a bandpass filter of 515-555 nm was used. Time resolution was  
54  
55  
56  
57  
58  
59  
60 at least 4 images per second.

1  
2  
3  
4 During  $\text{Ca}^{2+}$  imaging the PSS contained either 3  $\mu\text{M}$  wortmannin or 1  $\mu\text{M}$   $\alpha,\beta$ -mATP and 0.2  $\mu\text{M}$   
5  
6 prazosin which reduced contractions to field stimulation to less than 10% and consequently reduced  
7  
8 movement artifacts. In these experiments 3  $\mu\text{M}$  cocaine was present to inhibit NA uptake into the  
9  
10 varicosities.  
11  
12

13  
14  
15  
16 *Loading and imaging cell nuclei with Syto16.* To label nuclei the arteries mounted in the myograph  
17  
18 were incubated with 1  $\mu\text{M}$  Syto16 in PSS for 10 min at 37°C. After a wash in PSS, the arteries were  
19  
20 imaged with the Zeiss confocal microscope with the settings used for  $\text{Ca}^{2+}$  imaging.  
21  
22

23  
24  
25 *Measurement of NA release.* In artery segments mounted in myographs for isometric force  
26  
27 recording, NA release was measured using a MicroC™ Picoammeter/Potentiostat (WPI) with  
28  
29 nafion coated carbon fiber electrodes (diameter 30  $\mu\text{m}$ ; length 1 mm), across which a potential of  
30  
31 0.4 V was applied. The fiber electrodes were activated before use in accordance with the  
32  
33 instructions from the company. After mounting the arteries in the myograph, the mounting heads  
34  
35 and the artery were rotated to place the artery in a vertical position. Using a micromanipulator, the  
36  
37 electrode was placed alongside the artery, with the electrode gently touching the artery as judged  
38  
39 through the microscope. An Ag/AgCl electrode was used as reference electrode. Cocaine (3  $\mu\text{M}$ )  
40  
41 was present in all experiments. The signal was recorded simultaneously with force at 100 Hz. For  
42  
43 calibration of the signal, NA was applied to the myograph chamber in increasing concentrations  
44  
45 without an artery mounted in the myograph.  
46  
47  
48  
49  
50

51  
52  
53 *Solutions.* PSS contained (in  $\text{mmol L}^{-1}$ ): NaCl 119, KCl 4.7,  $\text{KH}_2\text{PO}_4$  1.18,  $\text{MgSO}_4$  1.17,  $\text{NaHCO}_3$   
54  
55 25,  $\text{CaCl}_2$  1.6, EDTA 0.026, glucose 5.5, was gassed with 5%  $\text{CO}_2$  in air or 5%  $\text{CO}_2/95\% \text{O}_2$   
56  
57 (during Oregon Green BAPTA-1 dextran loading) and had a pH of 7.4. In phosphate-free PSS  
58  
59  
60

1  
2  
3  
4 KH<sub>2</sub>PO<sub>4</sub> was omitted. In low K<sup>+</sup> solution KCl was reduced to 1.82 mM. ω-conotoxin GVIA was  
5  
6 obtained from Alomone Labs (Jerusalem, Israel); 4-AP, yohimbine, NA, ACh, ATP, α,β-methylene  
7  
8 ATP, TTX, prazosin, dendrotoxin, and charybdotoxin, and TEA were obtained from Sigma; cocaine  
9  
10 was from Aarhus University Hospital. The Ca<sup>2+</sup>-sensitive dyes and Syto16 were obtained from  
11  
12 Molecular Probes. Drug nomenclature is consistent with the Concise Guide to Pharmacology <sup>21</sup>.  
13  
14 During experiments the PSS was kept at 37°C.  
15  
16  
17  
18  
19

### 20 *Calculations and statistics.*

21  
22 Fluorescence in regions of interest (ROIs) placed in nerve fibers was used for analysis in the  
23  
24 Calcium Green-1-AM loaded arteries (5 to 10 ROIs per preparation) (Fig. 1A). In Oregon Green  
25  
26 488 BAPTA-1 dextran-loaded arteries ROIs encompassed single varicosities or intervaricose  
27  
28 segments (5 to 10 ROIs per preparation).  
29  
30  
31  
32  
33

34 Fluorescence intensity for ROIs was calculated as mean values of an interval of 3 s immediately  
35  
36 before activation and for the last 1 s of the activation. The mean intensity from a ROI was obtained  
37  
38 on all images of the stimulation series. Any movement of the ROI during the stimulation was  
39  
40 corrected for by an automated procedure, written in MatLab, which tracked the varicosity between  
41  
42 every frame based on the strongest local fluorescence signal compared with the background.  
43  
44 Background values were obtained from ROIs immediately outside the nerves and subtracted from  
45  
46 the values in the nerve specific ROIs.  
47  
48  
49  
50  
51

52 For each ROI, values during activation were expressed as the percentage of the value before  
53  
54 activation, and the data for all ROIs in the image were averaged. No calibration of the fluorescence  
55  
56 was made. The data obtained in the presence of CTX, 4-AP, yohimbine or ACh are expressed as the  
57  
58  
59  
60

percentage of the control values (i.e. without the drug) for individual ROIs and then averaged for the preparation.

The analysis of NA concentration and force was performed in a similar manner, i.e. by obtaining a baseline value in a 3 s period before activation and the value during the last 1 s of the activation.

The effects of drugs are expressed as percent of the baseline values.

Statistical analyses were made with Student's paired or unpaired *t*-test, two-way ANOVA, or extra sum-of-squares *F*-test as indicated. Data were expressed as mean±SEM, *n* is the number of arteries (one artery per rat) and *p*<0.05 was considered significant.

## ACKNOWLEDGEMENT

This work was supported by the Novo Nordic Foundation (# 11789 to C.A), The Danish Heart Foundation no (R97-A5232 to C.A.), Russian Foundation for Basic Research (#16-44-730649 to O.S.T.).

**CONFLICT OF INTEREST:** None declared.

## REFERENCES

1. Luff SE. Ultrastructure of sympathetic axons and their structural relationship with vascular smooth muscle. *Anat Embryol (Berl)*. 1996;193(6):515-531.
2. Brain KL, Bennett MR. Calcium in sympathetic varicosities of mouse vas deferens during facilitation, augmentation and autoinhibition. *J Physiol*. 1997;502 ( Pt 3):521-536.
3. Brain KL, Trout SJ, Jackson VM, Dass N, Cunnane TC. Nicotine induces calcium spikes in single nerve terminal varicosities: a role for intracellular calcium stores. *Neuroscience*. 2001;106(2):395-403.
4. Jackson VM, Trout SJ, Brain KL, Cunnane TC. Characterization of action potential-evoked calcium transients in mouse postganglionic sympathetic axon bundles. *J Physiol*. 2001;537(Pt 1):3-16.
5. O'Connor SC, Brain KL, Bennett MR. Individual sympathetic varicosities possess different sensitivities to alpha 2 and P2 receptor agonists and antagonists in mouse vas deferens. *Br J Pharmacol*. 1999;128(8):1739-1753.

- 1
  - 2
  - 3
  - 4
  - 5
  - 6
  - 7
  - 8
  - 9
  - 10
  - 11
  - 12
  - 13
  - 14
  - 15
  - 16
  - 17
  - 18
  - 19
  - 20
  - 21
  - 22
  - 23
  - 24
  - 25
  - 26
  - 27
  - 28
  - 29
  - 30
  - 31
  - 32
  - 33
  - 34
  - 35
  - 36
  - 37
  - 38
  - 39
  - 40
  - 41
  - 42
  - 43
  - 44
  - 45
  - 46
  - 47
  - 48
  - 49
  - 50
  - 51
  - 52
  - 53
  - 54
  - 55
  - 56
  - 57
  - 58
  - 59
  - 60
6. Lin YQ, Bennett MR. Varicosity-Schwann cell interactions mediated by ATP in the mouse vas deferens. *J Neurophysiol.* 2005;93(5):2787-2796.
  7. Lin YQ, Bennett MR. Schwann cells in rat vascular autonomic nerves activated via purinergic receptors. *Neuroreport.* 2006;17(5):531-535.
  8. Verkhratsky A, Steinhauser C. Ion channels in glial cells. *Brain Res Brain Res Rev.* 2000;32(2-3):380-412.
  9. Msgghina M, Gonon F, Stjärne L. Paired pulse analysis of ATP and noradrenaline release from sympathetic nerves of rat tail artery and mouse vas deferens: effects of K<sup>+</sup> channel blockers. *British Journal of Pharmacology.* 1998;125(8):1669-1676.
  10. Uhrenholt TR, Nedergaard OA. Calcium channels involved in noradrenaline release from sympathetic neurones in rabbit carotid artery. *Pharmacol Toxicol.* 2003;92(5):226-233.
  11. Nakamura K, Shimizu T, Tanaka K, Taniuchi K, Yokotani K. Involvement of presynaptic voltage-dependent Kv3 channel in endothelin-1-induced inhibition of noradrenaline release from rat gastric sympathetic nerves. *European Journal of Pharmacology.* 2012;694(1-3):98-103.
  12. Judge SIV, Bever Jr CT. Potassium channel blockers in multiple sclerosis: Neuronal Kv channels and effects of symptomatic treatment. *Pharmacology & Therapeutics.* 2006;111(1):224-259.
  13. Coetzee WA, Amarillo Y, Chiu J, et al. Molecular diversity of K<sup>+</sup> channels. *Annals of the New York Academy of Sciences.* 1999;868:233-285.
  14. Nielsen H, Pilegaard HK, Hasenkam JM, Mortensen FV, Mulvany MJ. Heterogeneity of postjunctional alpha-adrenoceptors in isolated mesenteric resistance arteries from rats, rabbits, pigs, and humans. *J Cardiovasc Pharmacol.* 1991;18(1):4-10.
  15. Artigues-Varin C, Richard V, Varin R, Mulder P, Thuillez C. Alpha2-adrenoceptor ligands inhibit alpha1-adrenoceptor-mediated contraction of isolated rat arteries. *Fundam Clin Pharmacol.* 2002;16(4):281-287.
  16. Peng H, Matchkov V, Ivarsen A, Aalkjaer C, Nilsson H. Hypothesis for the initiation of vasomotion. *Circ Res.* 2001;88(8):810-815.
  17. Mulvany MJ, Halpern W. Contractile properties of small arterial resistance vessels in spontaneously hypertensive and normotensive rats. *Circ Res.* 1977;41(1):19-26.
  18. Angus JA, Broughton A, Mulvany MJ. Role of alpha-adrenoceptors in constrictor responses of rat, guinea-pig and rabbit small arteries to neural activation. *J Physiol.* 1988;403:495-510.
  19. Nilsson H, Ljung B, Sjoblom N, Wallin BG. The influence of the sympathetic impulse pattern on contractile responses of rat mesenteric arteries and veins. *Acta Physiol Scand.* 1985;123(3):303-309.
  20. Nilsson H. Different nerve responses in consecutive sections of the arterial system. *Acta Physiol Scand.* 1984;121(4):353-361.
  21. Alexander SP, Kelly E, Marrion N, et al. The Concise Guide to PHARMACOLOGY 2015/16: Overview. *Br J Pharmacol.* 2015;172(24):5729-5743.

## LEGENDS TO FIGURES

Fig. 1. A) Loading of nerve fibers in rat mesenteric small arteries with Calcium Green-AM. The single arrow indicates an area of high dye intensity, where nerve fibers cross; the double arrow indicates area of lower dye intensity, which are nerve fibers. The red arrows indicate a smooth muscle cell, which is out of focus. Bar indicates 1  $\mu\text{m}$ . B) Traces (typical of 5 experiments) showing the effect of field stimulation at increasing frequencies (in Hz: 0.5, blue; 1, red; 2, violet 4, green; 16, light blue) on  $[\text{Ca}^{2+}]$  in nerve fibers (double arrow in fig. 1A). The insert shows the effect of 0.1  $\mu\text{M}$  tetrodotoxin (TTX) on 8 Hz field stimulation (typical of 3 experiments). C) and D) show two images of the same nerve fibers loaded with Calcium Green-AM before (C) and after (D) staining with Syto16. An area of high Calcium Green intensity where several nerve fibers cross is seen. In 20-30% of these areas, Syto16 gave a strong fluorescence demonstrating the presence of a nucleus. Images are typical of 4 experiments. Bars indicate 1  $\mu\text{m}$ . E) and F) Mean effect ( $n = 5$ ) of field stimulation at 2 Hz and 16 Hz under control conditions (grey bars) and in the presence of ATP (hatched bars). In E nerve fibers (double arrow in fig. 1A), and in F areas where nerves cross (single arrow in fig. 1A) were imaged. There was no significant difference between control and ATP, two-way ANOVA) for both E and F.

Fig. 2. The effect of 10  $\mu\text{M}$  ATP on nerve fibers loaded with Calcium Green-AM (column 1 and 2) or axons loaded with Oregon Green 488 BAPTA-1 dextran. The response of nerve fibers (column 1; double arrow in fig. 1A) or areas with high dye load (column 2; single arrow in fig. 1A) to bath application of ATP was measured. \*  $p < 0.05$ ; compared to fluorescence without ATP paired  $t$ -test;  $n=5$ .

1  
2  
3  
4  
5  
6  
7 Fig. 3. Effect of 100  $\mu\text{M}$   $\omega$ -conotoxin GVIA on  $[\text{Ca}^{2+}]_v$  in nerves as function of stimulation  
8 frequency in Calcium Green-AM loaded arteries. The responses to field stimulation are given as the  
9 percentage of the response at respective frequency in the absence of  $\omega$ -conotoxin GVIA,  $n=6$ .  
10  
11  
12  
13  
14

15  
16 Fig. 4. A) Image of axons in rat mesenteric small arteries loaded with Oregon Green 488 BAPTA-1  
17 dextran; bar indicates 1  $\mu\text{m}$ . B) Traces showing the effect of field stimulation at increasing  
18 frequencies (in Hz: 0.5, blue; 1, red; 2, violet 4, green; 16, light blue) on  $[\text{Ca}^{2+}]_v$  in Oregon Green  
19 488 BAPTA-1 dextran loaded axons. C) Traces showing the effect of a single pulse on Calcium  
20 Green-AM loaded nerve fibers (black trace) and Oregon Green 488 BAPTA-1 dextran loaded axons  
21 (violet). D) The effect of 10  $\mu\text{M}$  ATP on  $[\text{Ca}^{2+}]_v$  transients to field stimulation at 2 and 16 Hz in  
22 axons. \*  $p<0.05$ ; control vs. ATP two-way ANOVA,  $n=5$ .  
23  
24  
25  
26  
27  
28  
29  
30  
31  
32  
33

34 Fig. 5. Traces of noradrenaline release (top) and force (bottom) of rat mesenteric artery to field  
35 stimulation with frequencies of 2 Hz and 16 Hz under control conditions and in the presence of 10  
36  $\mu\text{M}$  4-aminopyridine.  
37  
38  
39  
40  
41  
42

43 Fig. 6. The average effect of field stimulation on  $[\text{Ca}^{2+}]_v$  (Oregon Green 488 BAPTA-1 dextran) (A,  
44  $n=14$ ), noradrenaline (NA) release (B,  $n=16$ ), and force (C,  $n=16$ ). The data plotted in B and C were  
45 recorded simultaneously from the same preparations. Data are given as the percentage of the  
46 response at 16 Hz.  
47  
48  
49  
50  
51  
52  
53

54 Fig. 7. Effects of 100 nM  $\omega$ -conotoxin GVIA (CTX), 10  $\mu\text{M}$  4-aminopyridine (4-AP), 1  $\mu\text{M}$   
55 yohimbine (Yoh), and 20  $\mu\text{M}$  acetylcholine (ACh) on  $[\text{Ca}^{2+}]_v$  (Oregon Green 488 BAPTA-1  
56  
57  
58  
59  
60



1  
2  
3  
4 dextran loaded axons) (A), noradrenaline release (B), and force (C) during 2 and 16 Hz stimulation  
5  
6 of rat mesenteric small arteries. The hatched bars are the responses in the presence of CTX.

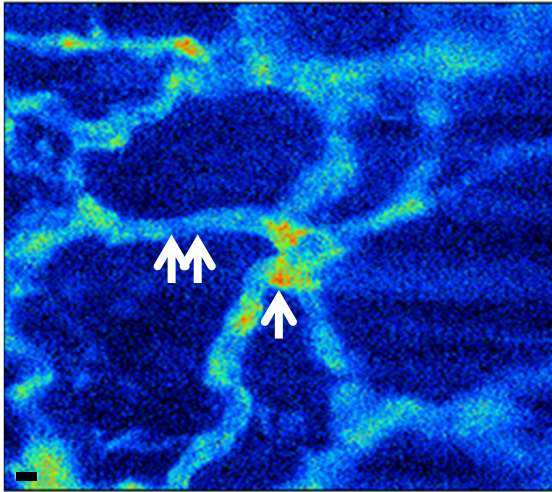
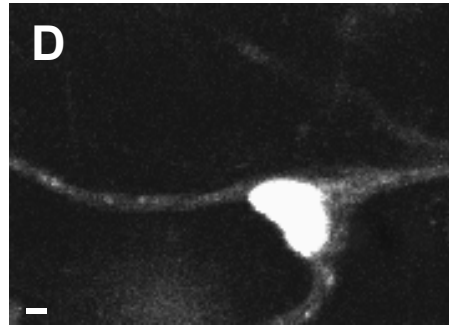
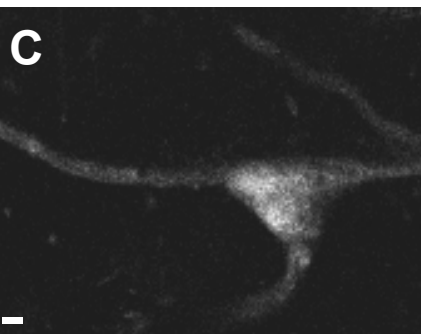
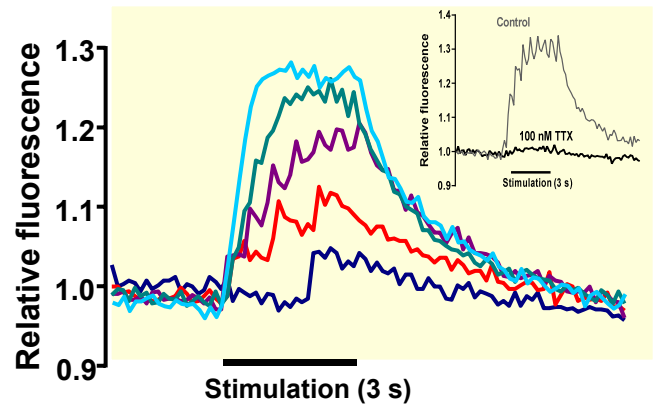
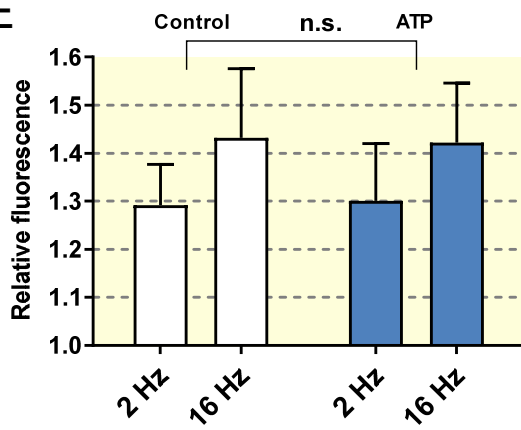
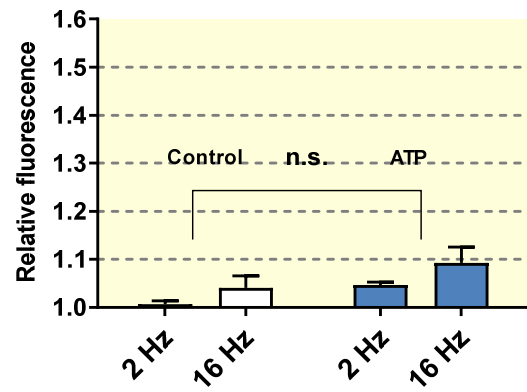
7  
8 Responses are given as the percentage of the responses of the same preparations at respective  
9  
10 frequency in the absence of drugs. \*  $p < 0.05$ ; paired  $t$ -test; different from 100 % (i.e. significant  
11  
12 effect of the drug); @  $p < 0.05$ ; unpaired  $t$ -test; different from the response in the presence of CTX  
13  
14 alone (i.e. effect of the drug in the presence of CTX);  $n = 3-8$ .  
15  
16  
17  
18  
19

20  
21 Fig. 8. Effects of 100 nM  $\omega$ -conotoxin GVIA (A,  $n = 5$ ), 10  $\mu$ M 4-AP (B,  $n = 5$ ), 1  $\mu$ M yohimbine (C,  
22  
23  $n = 5$ ) and 20  $\mu$ M ACh (D,  $n = 5$ ) on force development to exogenously applied noradrenaline. E  
24  
25 shows time-control (two consecutive concentration-response relationships obtained from the same  
26  
27 preparation,  $n = 4$ ). The responses were obtained in the presence of 3  $\mu$ M cocaine and given as the  
28  
29 percentage of the maximum response. \*  $p < 0.05$ ; extra sum-of-squares  $F$ -test.  
30  
31  
32  
33

34  
35 Fig. 9. Effect of 4-aminopyridine (4-AP), charybdotoxin, tetraethylammonium (TEA), and  
36  
37 yohimbine on 16 Hz field stimulation-induced noradrenaline release and tension development. A)  
38  
39  $n = 10$ ; B)  $n = 8$ . The columns represent cumulative addition of the drugs. \*  $p < 0.05$ ; paired  $t$ -test.  
40  
41

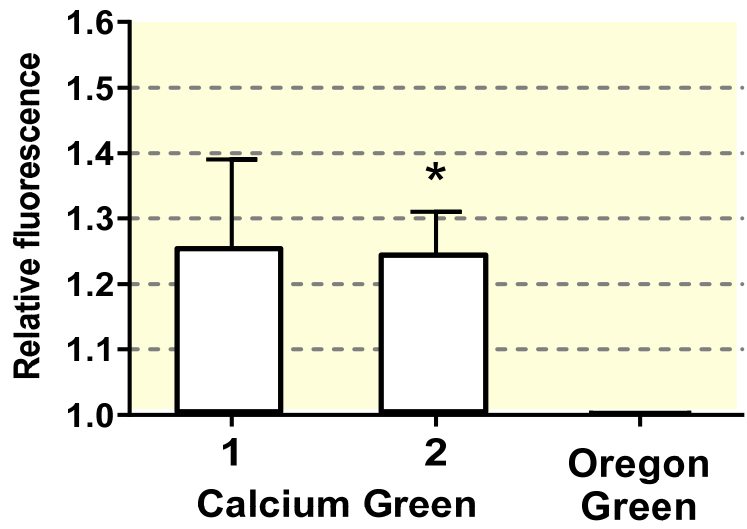
42  
43 **Suppl. Fig. 1. Staining of nerve fibers with Calcium Green-AM (A) and glyoxylic acid (B) in rat**  
44  
45 **mesenteric small arteries. In A cell nuclei are stained with Syto16. The preparation in A is shown as**  
46  
47 **a 3D structure in Suppl. Video 1. In Suppl. video 1 note that the nucleus marked with a double**  
48  
49 **arrow in (A) is in the nerve fiber, whereas the nucleus marked with a single arrow in (A) is outside**  
50  
51 **the nerve fiber. Bar indicates 4  $\mu$ m.**  
52  
53

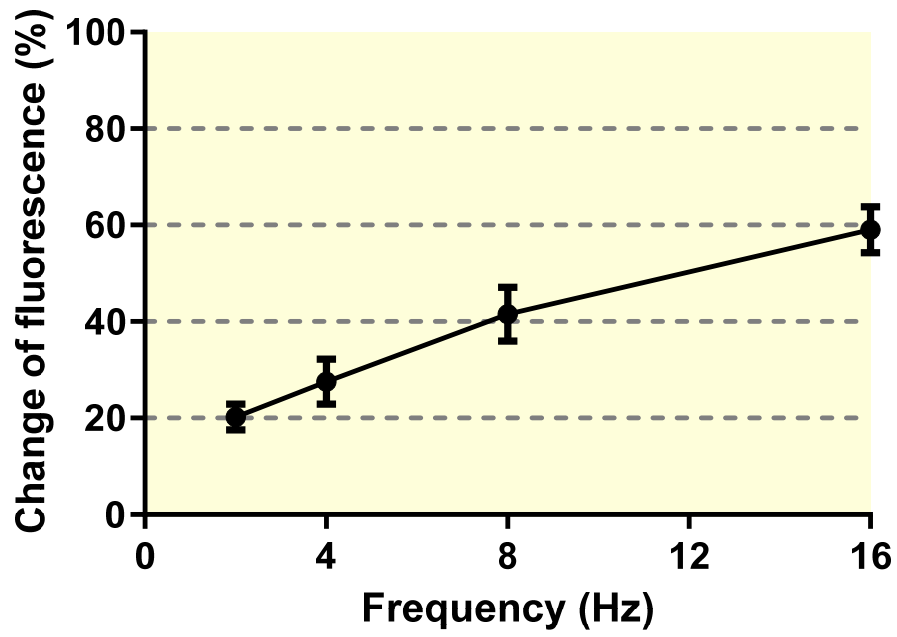
54  
55  
56 **Suppl. Video 1. A rat mesenteric small artery stained with Calcium Green-AM An image stack is**  
57  
58 **obtained with confocal microscopy and presented as a 3-D image.**  
59  
60

**A****B****E****F**

1  
2  
3  
4  
5  
6  
7  
8  
9  
10  
11  
12  
13  
14  
15  
16  
17  
18  
19  
20  
21  
22  
23  
24  
25  
26  
27  
28  
29  
30  
31  
32  
33  
34  
35  
36  
37  
38  
39  
40  
41  
42  
43  
44  
45  
46  
47  
48  
49  
50  
51  
52  
53  
54  
55  
56  
57  
58  
59  
60

1  
2  
3  
4  
5  
6  
7  
8  
9  
10  
11  
12  
13  
14  
15  
16  
17  
18  
19  
20  
21  
22  
23  
24  
25  
26  
27  
28  
29  
30  
31  
32  
33  
34  
35  
36  
37  
38  
39  
40  
41  
42  
43  
44  
45  
46  
47  
48  
49  
50  
51  
52  
53  
54  
55  
56  
57  
58  
59  
60

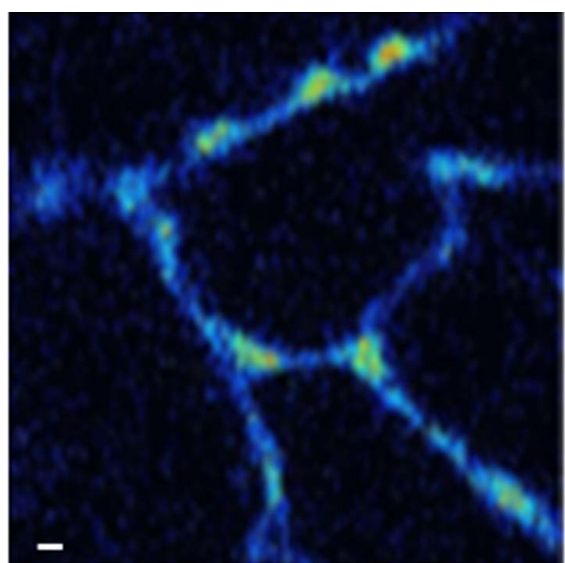




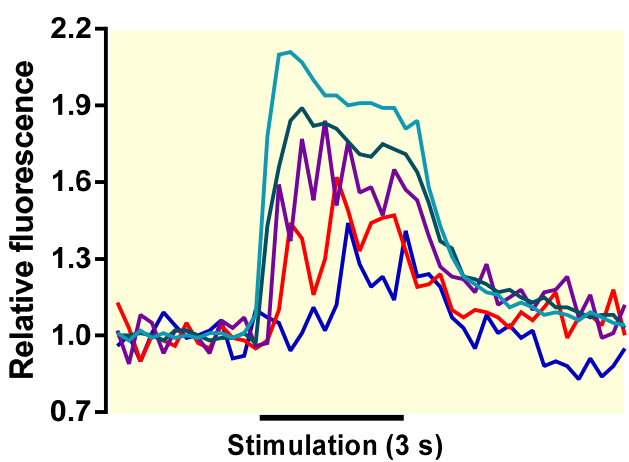
1  
2  
3  
4  
5  
6  
7  
8  
9  
10  
11  
12  
13  
14  
15  
16  
17  
18  
19  
20  
21  
22  
23  
24  
25  
26  
27  
28  
29  
30  
31  
32  
33  
34  
35  
36  
37  
38  
39  
40  
41  
42  
43  
44  
45  
46  
47  
48  
49  
50  
51  
52  
53  
54  
55  
56  
57  
58  
59  
60

1  
2  
3  
4  
5  
6  
7  
8  
9  
10  
11  
12  
13  
14  
15  
16  
17  
18  
19  
20  
21  
22  
23  
24  
25  
26  
27  
28  
29  
30  
31  
32  
33  
34  
35  
36  
37  
38  
39  
40  
41  
42  
43  
44  
45  
46  
47  
48  
49  
50  
51  
52  
53  
54  
55  
56  
57  
58  
59  
60

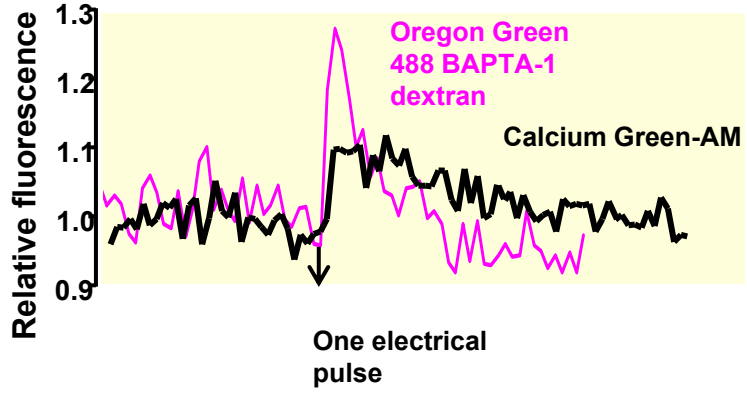
A



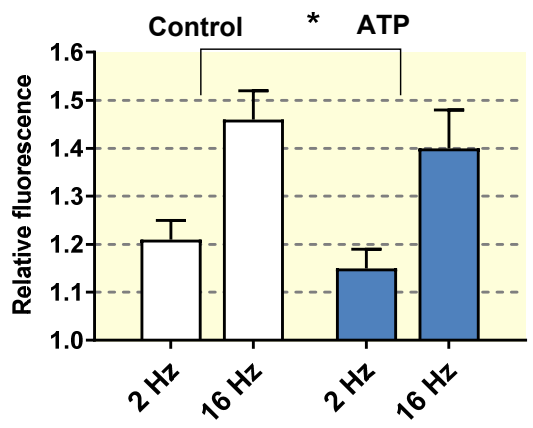
B

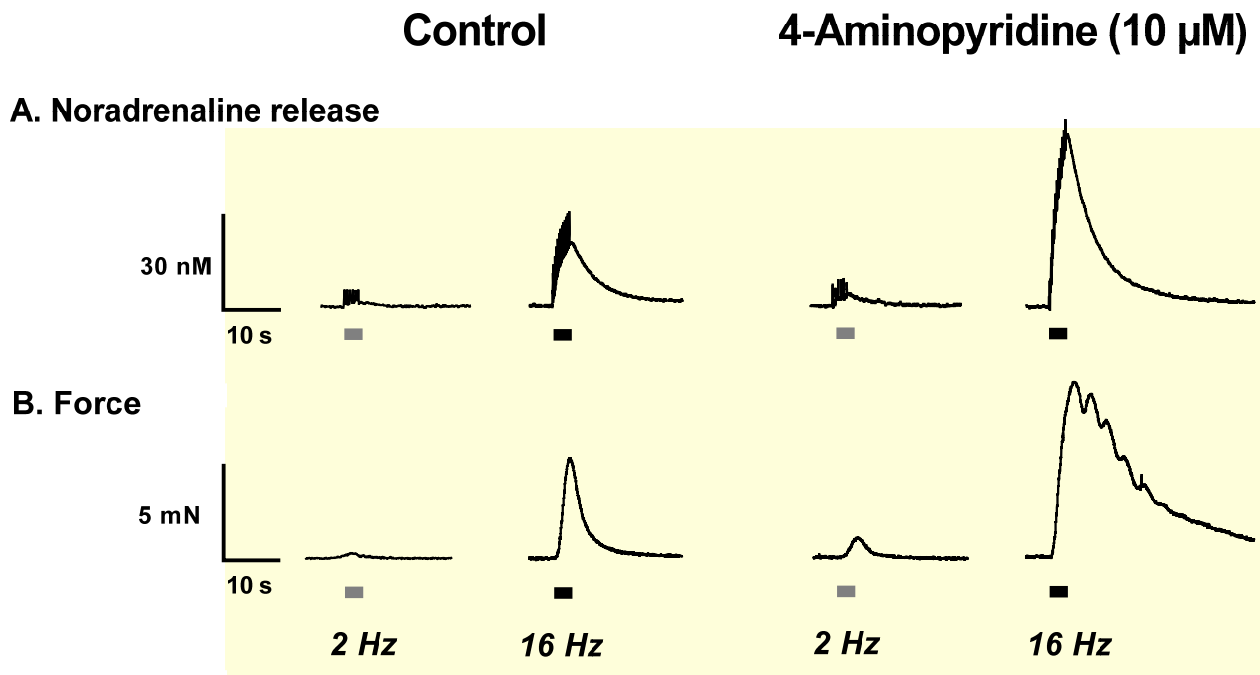


C

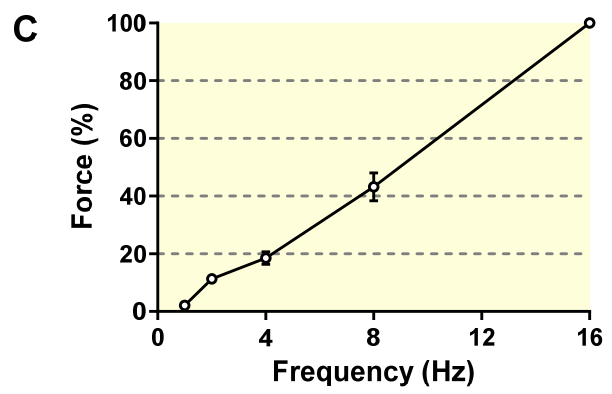
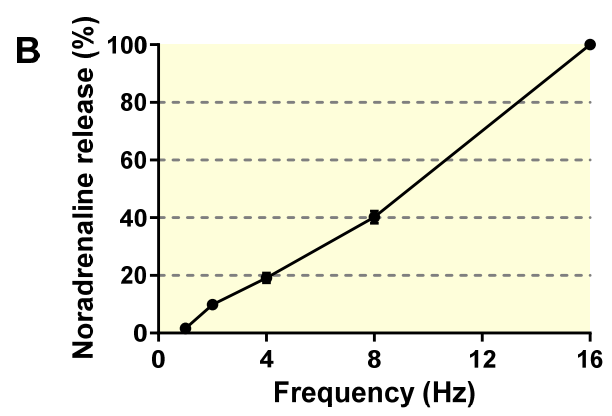
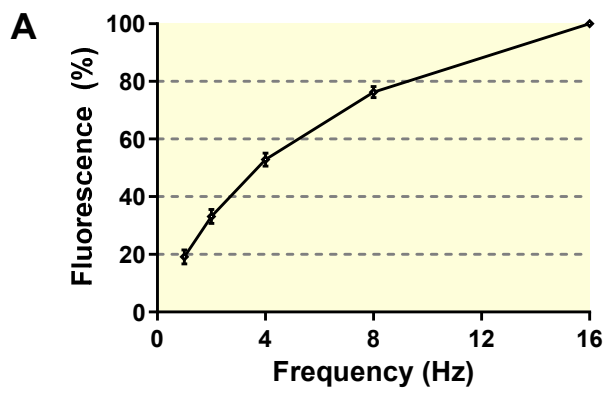


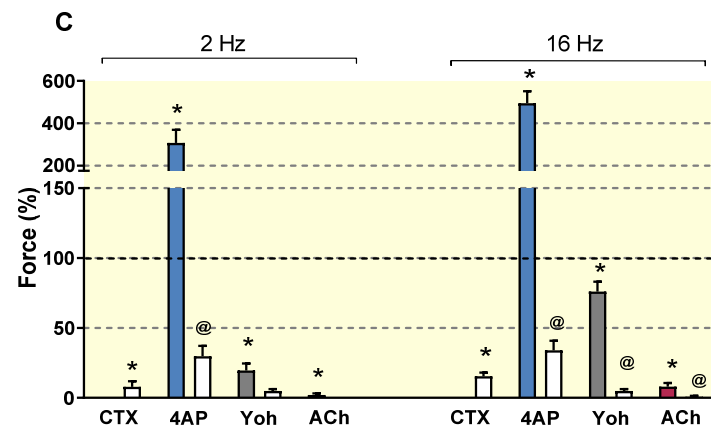
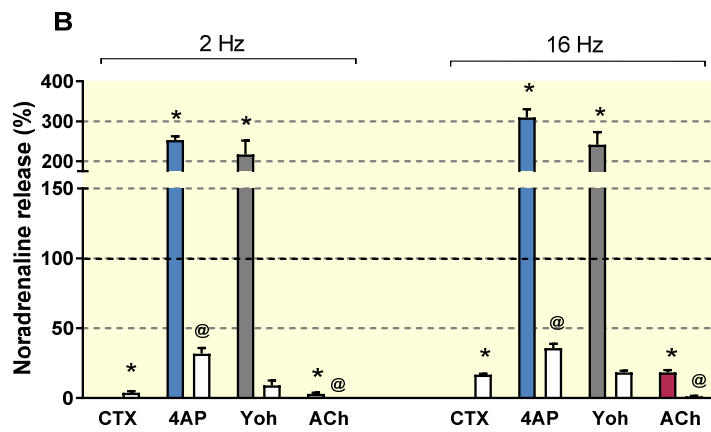
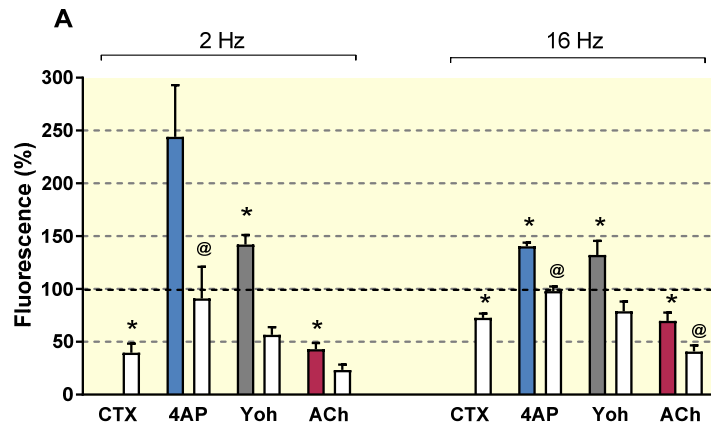
D





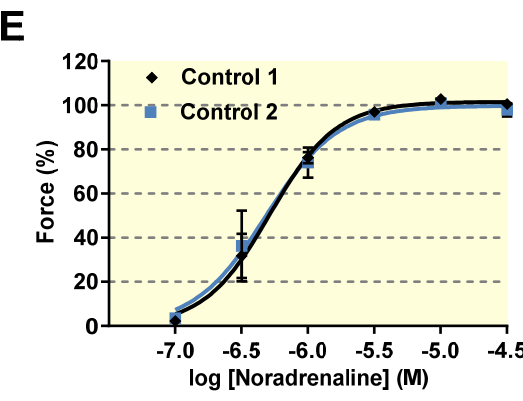
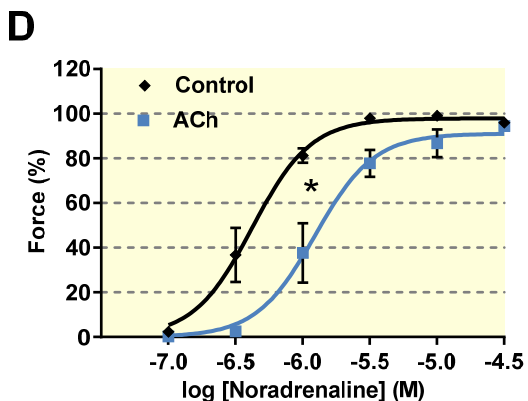
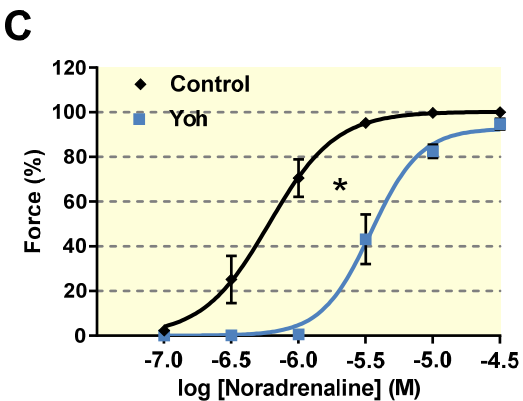
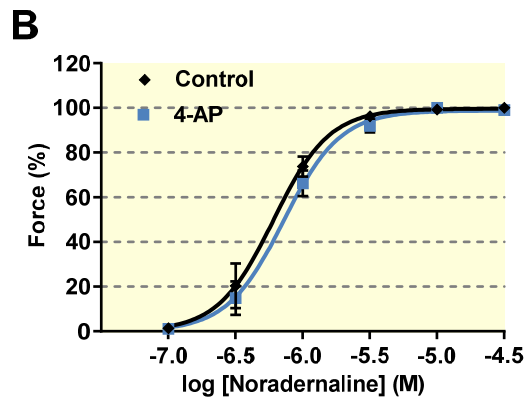
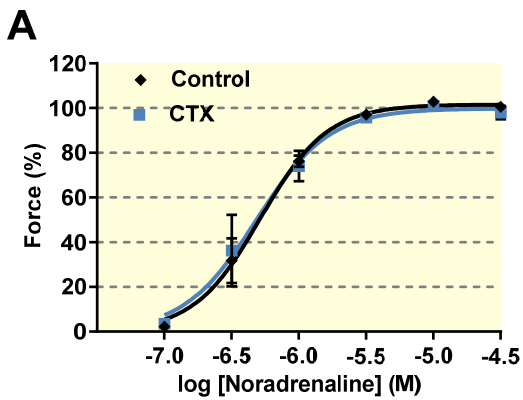
1  
2  
3  
4  
5  
6  
7  
8  
9  
10  
11  
12  
13  
14  
15  
16  
17  
18  
19  
20  
21  
22  
23  
24  
25  
26  
27  
28  
29  
30  
31  
32  
33  
34  
35  
36  
37  
38  
39  
40  
41  
42  
43  
44  
45  
46  
47  
48  
49  
50  
51  
52  
53  
54  
55  
56  
57  
58  
59  
60





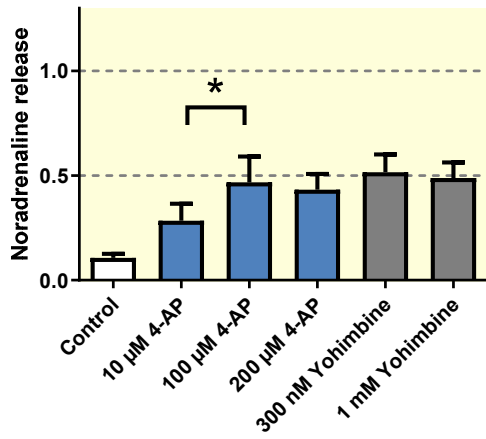
1  
2  
3  
4  
5  
6  
7  
8  
9  
10  
11  
12  
13  
14  
15  
16  
17  
18  
19  
20  
21  
22  
23  
24  
25  
26  
27  
28  
29  
30  
31  
32  
33  
34  
35  
36  
37  
38  
39  
40  
41  
42  
43  
44  
45  
46  
47  
48  
49  
50  
51  
52  
53  
54  
55  
56  
57  
58  
59  
60



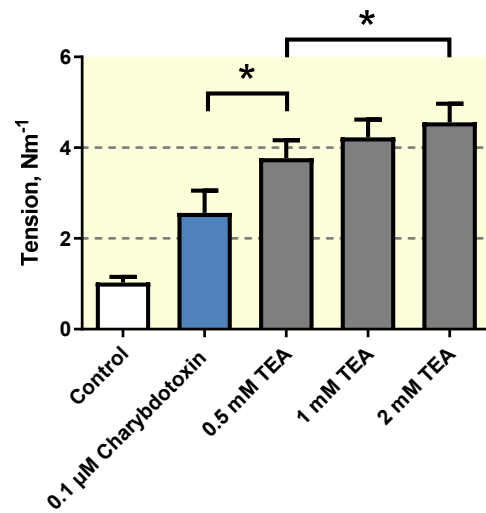
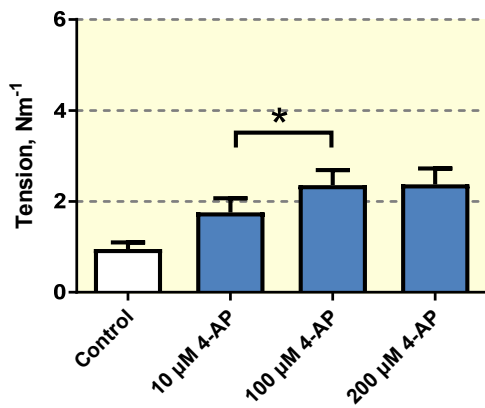
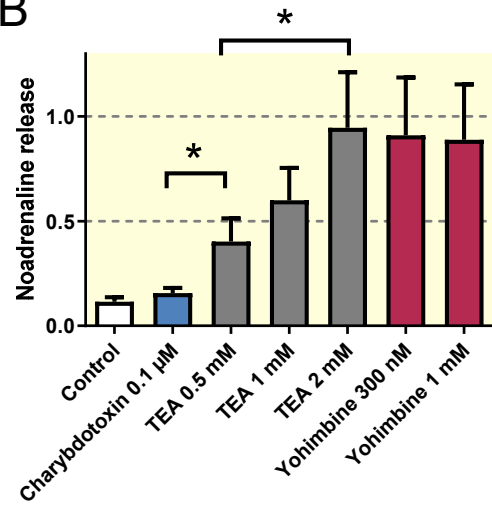


1  
2  
3  
4  
5  
6  
7  
8  
9  
10  
11  
12  
13  
14  
15  
16  
17  
18  
19  
20  
21  
22  
23  
24  
25  
26  
27  
28  
29  
30  
31  
32  
33  
34  
35  
36  
37  
38  
39  
40  
41  
42  
43  
44  
45  
46  
47  
48  
49  
50  
51  
52  
53  
54  
55  
56  
57  
58  
59  
60

A

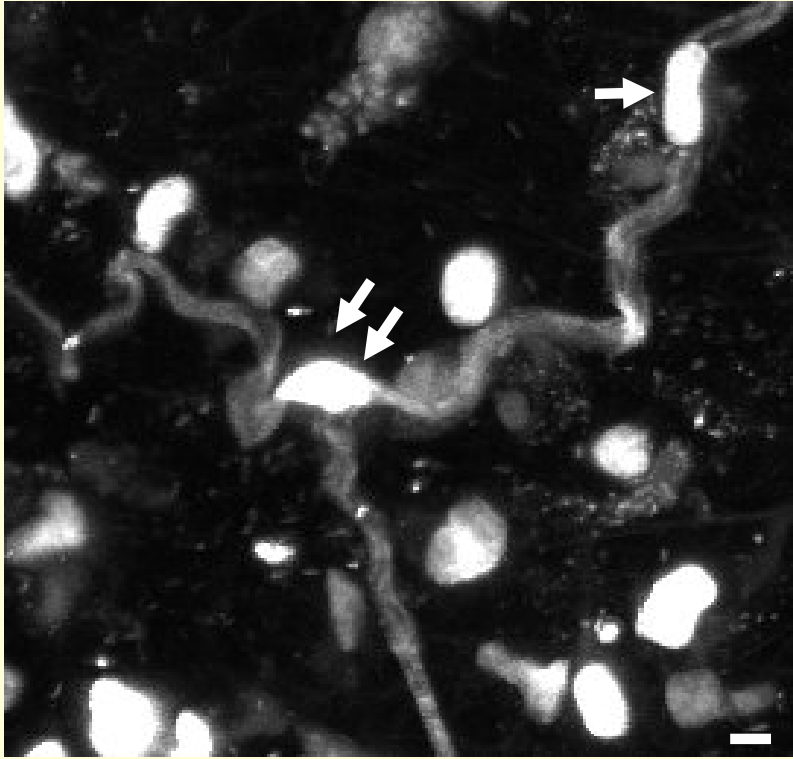


B

1  
2  
3  
4  
5  
6  
7  
8  
9  
10  
11  
12  
13  
14  
15  
16  
17  
18  
19  
20  
21  
22  
23  
24  
25  
26  
27  
28  
29  
30  
31  
32  
33  
34  
35  
36  
37  
38  
39  
40  
41  
42  
43  
44  
45  
46  
47  
48  
49  
50  
51  
52  
53  
54  
55  
56  
57  
58  
59  
60

1  
2  
3  
4  
5  
6  
7  
8  
9  
10  
11  
12  
13  
14  
15  
16  
17  
18  
19  
20  
21  
22  
23  
24  
25  
26  
27  
28  
29  
30  
31  
32  
33  
34  
35  
36  
37  
38  
39  
40  
41  
42  
43  
44  
45  
46

A



B

